

Dalton Transactions

Accepted Manuscript



This is an *Accepted Manuscript*, which has been through the Royal Society of Chemistry peer review process and has been accepted for publication.

Accepted Manuscripts are published online shortly after acceptance, before technical editing, formatting and proof reading. Using this free service, authors can make their results available to the community, in citable form, before we publish the edited article. We will replace this *Accepted Manuscript* with the edited and formatted *Advance Article* as soon as it is available.

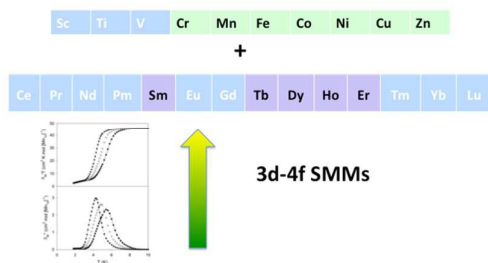
You can find more information about *Accepted Manuscripts* in the [Information for Authors](#).

Please note that technical editing may introduce minor changes to the text and/or graphics, which may alter content. The journal's standard [Terms & Conditions](#) and the [Ethical guidelines](#) still apply. In no event shall the Royal Society of Chemistry be held responsible for any errors or omissions in this *Accepted Manuscript* or any consequences arising from the use of any information it contains.

TOC content

This Dalton Perspectives gives an overview of what researchers want to achieve by preparing 3d-4f single-molecule magnets, the most significant results obtained so far and the challenges still ahead of us.

TOC graphic content



Cite this: DOI: 10.1039/x0xx00000x

Received 00th January 2012,

Accepted 00th January 2012

DOI: 10.1039/x0xx00000x

www.rsc.org/

Heterometallic 3d-4f Single Molecule Magnets

Lidia Rosado Piquer,^a E. Carolina Sañudo,^{*a}

The promising potential applications like information processing and storage or molecular spintronics of single molecule magnets (SMMs) have spurred the research of new, better SMMs. In this context, lanthanide ions have been seen as ideal candidates for new heterometallic transition metal-lanthanide SMMs. This Dalton Perspective reviews 3d/4f SMMs up to 2014 and highlights the most significant advances and challenges of the field.

Introduction

In the early 1990's the discovery that transition metal complexes could retain the magnetization caused an explosion of the field of coordination complexes. The first molecule that was shown to act as a magnet at the molecular level was a dodecanuclear complex of Mn(III)/Mn(IV) with acetato, oxo and water ligands, $[\text{Mn}_{12}\text{O}_{12}(\text{MeCOO})_{16}(\text{H}_2\text{O})_4]$, Mn_{12}Ac .¹ Molecules with this property were then called single molecule magnets (SMMs). Soon other transition metal complexes were also found to be SMMs, including a large family of Mn_{12} complexes with structures related to that of Mn_{12}Ac . Mn_{12}Ac , was the first SMM discovered and is still between the most studied. SMMs are by themselves already very interesting molecules with very special magnetic properties, but their discovery also brought in the possibility of application of SMMs in technological applications, substituting conventional ferromagnetic materials for SMMs. The promise of the use of SMMs in the processing and storage of information is not only that of the use of a new material for the same task, but that of opening the possibility of having ultra-high density information storage devices, or ultra-fast information processing devices based on SMMs. Additionally, as new SMMs are discovered, new applications are proposed as for example their use in molecular spintronics. There are two main problems that must be solved before all these proposals of technological applications of SMMs can be implemented. First, the working temperatures must be improved, so far all SMMs discovered to date only function at liquid helium temperatures, this in itself does not make them useless, but it greatly detains any such

applications in information storage and processing which is nowadays efficiently done with bulk ferromagnetic materials, or even spintronics. Second, in order to fabricate devices using SMMs, new technologies must be developed, so far there are only a few examples of SMMs for which surface deposition and addressing of single molecules has been explored. One can envision temperature not being an issue if the physical properties of the new SMMs should out-perform the classical magnets used today. Still, the issue of depositing and addressing a single molecule on a surface remains a great challenge for scientists working in the field.

The promise of the ultimate miniaturization of information storage and processing devices using SMMs has driven many researchers' efforts in obtaining new improved examples of SMMs. In particular, the main goal has been to obtain SMMs with higher working temperatures, but there are still many different ways in which researchers report the success of the new SMMs, a useful parameter would be the blocking temperature. The blocking temperature, TB, the maximum temperature at which the SMM is functional, should be the temperature at which magnetization hysteresis vs. field is observed. The use of the blocking temperature is greatly hampered due to the fact that its value greatly depends on the sweep-rate of the magnetic field during the measurement and on the experiment used to measure it, so when comparing blocking temperature values one should be extremely careful. When characterizing SMMs the effective barrier for reversal of the magnetization, U_{eff} , is most often reported in the literature. This is also called the anisotropy barrier and it is the energy needed to transform the SMM in a simple paramagnet. U_{eff} is the most popular parameter used to characterise SMMs, mainly

due the phenomenon of quantum tunnelling of the magnetization, of particular importance for 3d-4f SMMs. For a complex to be a good SMM with high blocking temperature, U_{eff} must be large. Several researchers proposed ways in which to normalise the parameters that should be reported for each new SMM. Long and co-workers proposed that the temperature at which 1/2 width hysteresis is observed should be reported, while Sessoli and co-workers propose to define the blocking temperature as the temperature at which the magnetisation relaxes in 100 s. However, neither of these two definitions is widely used by scientists in the field and U_{eff} is still the parameter that is usually reported. In part, this is due to the fact that most reported SMMs do not display hysteresis of the magnetization above 1.8 K, the lower limit in temperature for commercial SQUID magnetometers, thus access to lower temperatures is required to perform hysteresis vs. field measurements to obtain TB. The Mn_{12} family of SMMs, with an $S = 10$ ground state were the SMMs with the highest blocking temperatures ($TB = 3.5$ K) and U_{eff} values up to 74 K^2 until 2007, when Brechin a co-workers reported a Mn_6 complex with a record U_{eff} of 86.4 K and $S = 12$.³ Thus, many SMMs have been reported since Mn_{12}Ac but reported working temperatures still remain in the liquid helium regime. If anisotropy barriers are compared the case is similar, and the reported values are not that much greater than that of Mn_{12}Ac . The anisotropy barrier for the reversal of the magnetization in transition metal SMMs depends on two properties: the total spin of the molecule S and the Ising-type anisotropy, gauged by the zero-field splitting parameter D and is defined as $U_{\text{eff}} = S^2 |D|$ or $U_{\text{eff}} = (S^2 - 1/4) |D|$ for integer and half integer spins respectively. This knowledge has been used to design improved SMMs based on two strategies: rising S and increasing the anisotropy of the molecule. Increasing S by introducing stronger ferromagnetic coupling has been achieved in several examples, but with more complex structures, a large S value has not been accompanied by a large molecular anisotropy: examples are Mn_{18} ,⁴ Mn_{21} ,⁵ Mn_{84} ⁶ or Mn_{19} .⁷ Particularly the latter, Mn_{19} possess the record spin of $83/2$ for a molecular cluster, but it lacks anisotropy and thus it is not an SMM. Focus is set now in increasing the magnetic anisotropy of the prepared complexes in order to improve SMM properties. In this context lanthanides seem a great choice for obtaining better SMMs: the lanthanide ions (and also the actinides) possess huge single-ion anisotropies. In 2003, the first mononuclear SMMs were reported and they contained a lanthanide ion. Ishikawa and co-workers reported mononuclear $\text{TBA}[\text{Ln}(\text{Pc})_2]$ complexes⁸ which were the first mononuclear SMMs and the first lanthanide SMMs. The $\text{TBA}[\text{Ln}(\text{Pc})_2]$ complex displayed frequency dependent ac out-of-phase peaks as high as 40 K and had energy barriers of $U_{\text{eff}}=230 \text{ K}$ and $U_{\text{eff}} = 28 \text{ K}$ with $\text{Ln}=\text{Tb}$ and $\text{Ln}=\text{Dy}$ respectively. After this ground-breaking developments, the quest for improved SMMs took a new approach: to combine 3d and 4f metal centres in the

same complex to obtain SMMs that would have higher working temperatures than those obtained for 3d metal SMMs.

As of August 2014, in the Cambridge Crystallographic Data Base there are 1632 hits of Ln-oxo-3d (3d = V, Cr, Mn, Fe, Co, Ni, Cu) compounds, including MOFs, polymeric structures and salts. Of these, about 387 research papers report heterometallic molecular complexes containing 3d metals and lanthanide ions, in many instances each paper reports several crystal structures or a family of 3d-4f complexes where usually the lanthanide is changed in each complex. In nearly 100 of these publications, 3d-4f SMMs are reported and it is most usually the Tb(III) and Dy(III) complexes those which display SMM properties. This Dalton Perspectives gives an overview of what researchers want to achieve by preparing 3d-4f SMMs, the most significant results obtained so far and the challenges still ahead of us.

3d-4f SMMs: exploiting the magnetic properties of the 4f ions

If controlling the spin is a hard task for experimental chemists, controlling the anisotropy of a high nuclearity complex is even more complicated. Initially, complexes of the more anisotropic transition metals, known to display strong axial anisotropy like Mn(III), Co(II) and Ni(II) were investigated, and still are, as a means to obtain better SMMs. However, in the early 2000's the search for 3d-4f SMMs became an important trend, with the goal of improving the anisotropy of the obtained species and thus obtaining better SMM properties. The lanthanide ions are well known for having strong spin-orbit coupling, their magnetic properties ruled by the quantum number J , which has the maximum value of $|L + S|$ for lanthanides with more than half-filled f -shell (Tb, Dy, Ho, Er, Tm, Yb, Lu) and the minimum value of $|L - S|$ for lanthanides with less than half-filled f -shell (Ce, Pr, Nd, Pm, Sm, Eu). The number of unpaired electrons has little impact in the magnetic moment of the lanthanide ion and those with large m_J value of the ground state are the ones with stronger magnetic moment. The ground-state bi-stability characteristic of an SMM arises in lanthanide ions from the m_J sublevels of the $^{2S+1}L_J$ term. The most common lanthanide ions used to obtain SMMs are terbium(III) and dysprosium(III), but also erbium(III), samarium(III), ytterbium(III), gadolinium(III) and holmium(III). As Ishikawa showed for the Tb and Dy sandwich phthalocyanin complexes reported in 2003,⁸ in lanthanide SMMs the energy barrier is defined by the spin and angular momentum of a single lanthanide placed in a ligand field giving the largest $|Jz|$ the lowest energy and a large energy gap to the next sublevels. Long and Rinehart proposed simple rules in order to exploit the lanthanides single-ion anisotropy for designing 4f SMMs.⁹ According to their theory, to maximize the anisotropy of oblate ions (Ce(III), Pr(III), Nd(III), Tb(III), Dy(III) and Ho(III)) the crystal field should be such that the ligand electrons are concentrated above and below the xy plane. On the other hand,

for prolate ions (Pm(III), Sm(III), Er(III), Tm(III) and Yb(III)) an equatorial coordination geometry is preferred. Many of the reported 4f SMMs follow this prediction, and it is particularly useful for mononuclear lanthanide SMMs. This simple qualitative way of predicting SMM behaviour could also be used to ascertain whether a lanthanide ion in a 3d-4f complex will contribute strongly to the complex anisotropy, and thus, to the SMM properties of the 3d-4f species. However, this must be only considered in a very qualitative manner. Given the difficulties in factoring out all of the contribution to a polynuclear complex's magnetic anisotropy, the relationship between the ligand arrangement around the lanthanide ion in a 3d-4f polynuclear complex and the complex's axial anisotropy will not be as straight forward as with mononuclear lanthanide SMMs. Ideally, the most anisotropic 3d metals should be combined with the right lanthanide to obtain new SMMs: the anisotropy of the 3d-4f complex will be a combination of the single ion anisotropies of all the paramagnetic metal centres involved. A huge advantage of the lanthanide ions is the possibility of preparing families of complexes in which the properties of the 3d metal core can be checked, for example using the diamagnetic Y(III) or the lanthanides La(III) or Lu(III), with similar ionic radius or the isotropic Gd(III). In this way, one can check the contribution to the SMM property from the 3d metals in the molecule. For example, the family of complexes **5** in Table 1,¹⁰ where the **5**(La) without 4f electrons or anisotropy provided by the lanthanide ion is an SMM, indicating that the [Mn₆] core of the molecule is the main contribution to the anisotropy. Using a diamagnetic 3d metal analogue might be feasible, as many researchers have done in the past for different reasons. Metals in the oxidation state +3 can be replaced by Ga(III)¹¹ and metals in the oxidation state +2 can be replaced by diamagnetic Zn(II), however, these are more complicated reactions than replacing a lanthanide for Gd(III) or La(III), and one must not give for granted that it will be possible to study the Ln(III) in the cluster environment without the 3d electrons or anisotropy of the 3d single ions.

So far, the magnetic coupling between 4f and 3d metals has not been mentioned. It has been tacitly understood that for better SMMs the magnetic coupling between the metal centres in the complex should be strong and ferromagnetic to provide isolated ground states and avoid mixing of low-lying excited states that can provide ways for QTM to occur. Perhaps this is one of the biggest problems of 3d-4f complexes as SMMs: the magnetic coupling between transition metals and lanthanide ions is generally weak or very weak. Monoatomic oxo bridges are the surest way to enforce the strongest possible coupling. Usually, 3d-4f exchange constants have values below 5 K. A great tool to elucidate 3d-4f magnetic coupling is the software PHI,¹² which was especially conceived to treat magnetic data for systems containing lanthanide ions through the inclusion of spin-orbit coupling and crystal field effects, even though it is computationally demanding for high nuclearity complexes. The

qualitative approach developed by Rinehart and Long⁹ could be of use when excited states must be considered, the Dy(III) first excited states also have oblate-like shapes and could thus contribute to SMM behaviour in a coupled 3d-4f complex. However, that would not be the case for Tb(III) 3d-4f SMMs, since the excited terms are not oblate in shape.

Characterization of 3d-4f SMMs

As for any SMM, 3d-4f SMMs are usually characterized in their pure crystalline form using commercial SQUID magnetometers. The usual measurements of susceptibility against temperature and magnetization against field are also performed for 3d-4f SMMs. With these data, usually reported as the χT product and the reduced magnetisation one can evaluate the magnetic coupling between the metal centres in the complex as well as the spin ground state. For 3d-4f complexes, this is by no means straightforward and in many it will not be possible to quantify the magnetic exchange. For SMMs, alternate current (ac) magnetic susceptibility is also measured. Usually a small magnetic field of 1-5 Oe that oscillates at frequencies between 1 and 1500 Hz is used to measure magnetic susceptibility over a range of temperatures. For an SMM each individual molecule has an energy barrier to be overcome in order to reverse the magnetic moment, the SMM molecules will freeze and lag behind the applied ac field resulting in a susceptibility signal with two components: one in-phase with the ac oscillating field χ' and one out-of-phase with the oscillating field χ'' . The appearance of out-of-phase maxima that are frequency dependent is the most reliable signature of SMM behaviour. A typical example is shown in Figure 1. These experiments are usually performed scanning the temperature and frequency domains, resulting in susceptibility vs. T and susceptibility vs. frequency plots. From the slope of the plot of $\ln \tau$ vs $1/T$ one can obtain the anisotropy barrier where the graph is linear using an Arrhenius' type of equation, $\tau = \tau_0 \exp(-U_{eff}/kT)$. For lanthanide SMMs a temperature independent region is usually observed that is characteristic of fast relaxation of the magnetisation via quantum tunnelling (QTM). When the thermal mechanism coexists with the QTM, a curvature is seen in the Arrhenius' plot of $\ln \tau$ vs $1/T$. Several thermal relaxation processes can also coexist, and this can be assessed by examination of so called Argand or Cole-Cole plots. In these plots, χ'' is plotted against χ' at a constant temperature, resulting in a semi-circular representation. When a distribution of energy barriers exists the semicircle is distorted, a Debye model applies and the parameter α gages the distribution. Usually for SMMs this parameter has values smaller than 0.2.

Table 1. 3d-4f SMMs. The effective barriers measured with an applied dc field have the field value in Oe in parenthesis.

	Formula	U _{eff} (K)	TB (K)	Ref.
1	[CuLn(hfac) ₂] ₂ (Ln = Tb, Dy)	2.1	1.2	19
2	[Dy ₆ Mn ₆ (H ₂ shi) ₄ (Hshi) ₂ (shi) ₁₀ (MeOH) ₁₀ (H ₂ O) ₂]			20
3	[Mn ₁₁ Dy ₄ O ₈ (OH) ₆ (OMe) ₂ (O ₂ CPh) ₁₆ (NO ₃) ₅ (H ₂ O) ₃]	9.3		21
4	[Mn ₁₈ DyO ₈ (Cl) _{6.5} (N ₃) _{1.5} (HL) ₁₂ (MeOH) ₆]Cl ₃		0.5	23
5	[PrNH ₂] ₃ [Mn ₆ LnO ₃ (OMe) ₃ (SALO) ₆ (SALOH) ₃] (Ln = La, Dy, Tb)	6; 1.3		10
6	[M ₂ (L) ₂ (PhCOO) ₂ Dy ₂ (hfac) ₄] (M = Zn, Co)	47.9; 8.8		26
7	[Co ₂ Dy ₂ (OMe) ₂ (teaH) ₂ (Piv) ₆]	51; 127		29
8	[Dy ₂ Co ₂ (OMe) ₂ (L) ₂ (OOCPh) ₄ (MeOH) ₄ (NO ₃) ₂] (L = teaH, dea, mdea, bdea)	87, 104		31
9	[Dy ₂ Co ₂ (OMe) ₂ (L) ₂ (OOCPh) ₄ (MeOH) ₂ (NO ₃) ₂] (L = mdea, tea, bdea)	79, 115		31
10	[Dy ₂ Co ₂ (OMe) ₂ (teaH) ₂ (OOCPh) ₄ (MeOH) ₂ (NO ₃) ₂]	88		32
11	[Cr ₂ Dy ₂ (OMe) ₂ (Rdea) ₂ (acac) ₄ (NO ₃) ₂] (R = Me, Et, tBu)	34, 37, 41	1.8, 2.2, 2.2	33
12	[Cr ₂ Dy ₂ (OMe) ₂ (O ₂ CPh) ₄ (mdea) ₂ (NO ₃) ₂]	77	2.2	33
13	[Dy ₂ Mn ₂ (OH) ₂ (CymCOO) ₈ (THF) ₄]			34
14	[Ni ₂ Dy ₂ (L) ₄ (NO ₃) ₂ (S) ₂] (S = MeOH, DMF)	21.3; 18.5	4.2; 3.2	35
15	[Co ₂ Dy ₂ (L) ₄ (NO ₃) ₂ (THF) ₂]	82	3	36
16	[Mn ₃ Ln ₄ (O) ₆ (mdea) ₂ (mdeaH) ₂ (Piv) ₆ (NO ₃) ₄ (H ₂ O) ₂] (Ln = Dy, Ho, Y)	38.6	1.9	37
17	[Mn ₂₁ DyO ₂₀ (OH) ₂ (tBuCOO) ₂₀ (HCOO) ₄ (NO ₃) ₃ (H ₂ O) ₇]	74	3	38
18	[Dy ₁₀ Co ₂ (L) ₄ (MeCOO) ₁₆ (SCN) ₂ (MeCN) ₂ (H ₂ O) ₄ (OH) ₆]·2Co(SCN) ₄	4.3; 25		39
19	[H ₂ O][Cu ₂₄ Dy ₈ (Ph ₃ CPO ₃) ₆ (Ph ₃ CPO ₃ H) ₆ (MeCOO) ₁₂ (MeCOOH) ₆ (OH) ₄₂ (NO ₃)(OH) ₆]	4.6	0.6	40
20	[Mn ₉ Dy ₈ O ₈ (OH) ₈ (tea) ₂ (teaH) ₂ (teaH ₂) ₄ (MeCOO) ₄ (NO ₃) ₂ (H ₂ O) ₄](NO ₃) ₇			41
21	[Mn ₆ O ₃ (saO) ₆ (MeO) ₆ Ln ₂ (MeOH) ₄ (H ₂ O) ₂] (Ln = Tb, La)	103; 32.8	3.1; 8.7	45
22	[Ln ₂ Mn ₆ O ₃ (OMe) ₄ (Et-saO) ₆ (acac) ₂ (S) ₄] (Ln = Gd, S = MeOH; Tb, S = 3 MeOH 1 EtOH)	24; 46		46
23	[Ln ₆ Mn ₁₂ O ₇ (OH) ₁₀ (MeCOO) ₁₄ (mpea) ₈] (Ln = Tb, Gd)	36.6		47
24	[Tb ₆ Mn ₁₂ O ₉ (OH) ₈ (MeCOO) ₁₀ (mpea) ₈ (mp) ₂ (MeOH) ₂ (H ₂ O) ₂]	19.6		47
25	[Mn ₅ Tb ₄ O ₆ (mdea) ₂ (mdeaH) ₂ (Piv) ₆ (NO ₃) ₄ (H ₂ O) ₂]	33		37
26	[Mn ₃ Ln ₄ (mosao) ₂ (mosaoH) ₄ (piv) ₄ (N-mdea) ₄] (Ln = Y, Tb)	13.83		48
27	[LnCu ₄ (L) ₂ (OH) ₄ (H ₂ O) ₈ (NO ₃) ₂](ClO ₄) ₂ (Ln = Tb, Sm)	25		49
28	[(CuL) ₂ Tb(H ₂ O)(NO ₃) ₃]	20.3		50
29	[{(CuL) ₂ Tb(H ₂ O)(NO ₃) ₃ } ₂ bpy]	18		50
30	[TbCu ₃ (H ₂ edte)(NO ₃)](NO ₃) ₂	19.3 (1000)	1.6	52
31	[Cu ₃ Tb(Lbu)(NO ₃) ₂ (MeOH)(H ₂ O)](NO ₃)	19		53
32	[Cu(H ₂ L)(MeOH)] ₂ Tb(H ₂ O) _{0.57} (DMF) _{0.43} Fe(CN) ₆	13		54
33	[Cu ₆ Tb ₂ (L) ₄ (NO ₃) ₃ (MeCOO) ₂ (MeOH) ₅]NO ₃	15.6		55
34	[LCu(O ₂ COMe)Tb(thd) ₂]	13	0.7	56
35	[Ln ₂ Ni ₄ L ₂ Cl ₂ (OH) ₂ (MeO) ₂ (MeOH) ₆]Cl ₂ (ClO ₄) ₂ (Ln = Tb, Y)	30		57
36	[{L ₂ Ni(H ₂ O)Tb(dmff) _{2.5} (H ₂ O) _{1.5} } ₂ {W(CN) ₈ }]	15		58
37	[Fe ₁₂ Ln ₄ O ₁₀ (OH) ₄ (PhCO ₂) ₂₄] (Ln = Sm, Gd)	16	0.5	59
38	[Mn ₄ Ln ₄ (nBudea) ₄ (HCOO) ₄ (OMe) ₄ (OOCt) ₈ (MeOH) ₄] (Ln = Sm, Y)	12 (2000); 12	1	61
39	{(CO ₃) ₂ [Zn(L)Ln(H ₂ O)] ₂ }(NO ₃) ₂ (Ln = Tb, Dy, Er, Yb)	19 (1000)		70
40	[Zn(L)(NO ₃)Ln(NO ₃) ₂] (Ln = Tb, Dy, Er, Yb)	27 (1000)		70
41	[Ln ₂ Mn(C ₇ H ₅ O ₈) ₈] Ln = Tb, Dy	19, 92		73

Researchers still have a lot to learn from new lanthanide SMMs,²⁵ including the occurrence of multiple relaxation processes for pure SMM,⁷¹ and the toroidal magnetic moment in some 4f SMMs,⁷² among others. The phenomena of multiple relaxation processes and the QTM also occur in transition metal SMMs.

Magnetisation vs. field hysteresis loops can be measured in commercial SQUID magnetometer down to 1.8 K or using a micro-SQUID or micro Hall probe with suitable sweep rates for the field, going down to the mK regime. Due to the fact that most 3d-4f SMMs display hysteresis of the magnetisation vs. field at very low temperatures, when possible micro-SQUID data are reported. Blocking temperatures and anisotropy

barriers can be obtained from magnetisation decay measurements, performed also using a micro-SQUID. X-ray magnetic circular dichroism (XMCD) is a technique that has been used in few occasions to analyse magnetic behaviour of 3d-4f complexes. XMCD is element sensitive and can be used to probe the magnetism of each metal type in an heterometallic complex. Pedersen and co-workers published a great example in 2012, where they reported element specific curves for a Cr-Dy complex.¹³ XMCD could be exploited for evaluating the 3d-4f coupling in heterometallic complexes. Furthermore, XMCD can also be used to probe the magnetic properties of the SMM on a surface, a key and challenging step for physicists and chemists, as we reported for a Dy MOF of SMMs¹⁴ and that

Sessoli and co-workers pioneered with their work on Mn_{12}^{15} and $\text{Fe}_4^{16,17}$ SMMs on surfaces.¹⁸

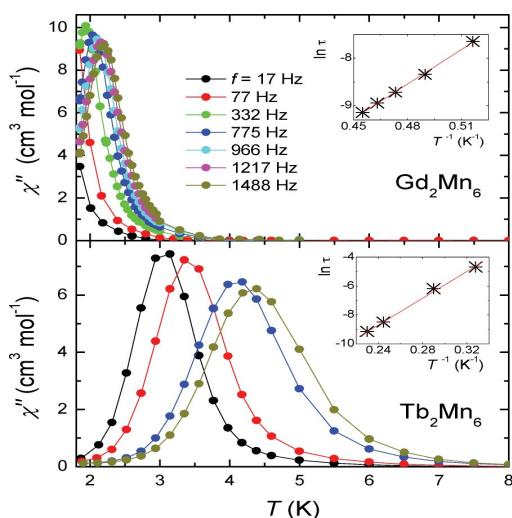


Figure 1. Typical ac magnetic susceptibility data and Arrhenius plot for a 3d-4f SMM. Reproduced from ref. 46 with permission from the Royal Society of Chemistry.

A wide perspective on 3d-4f SMMs

The first 3d-4f SMMs were reported in 2004: $[\text{CuLLn}(\text{hfac})_2]_2$ (**1**, Ln = Tb, Dy; $\text{H}_3\text{L} = 1-(2\text{-hydroxybenzamido})-2-(2\text{-hydroxy-3-methoxybenzylideneamino})\text{-ethane}$)¹⁹ squares with the 3d and 4f metal in an alternated array reported by Matsumoto *et al.*, and complex $[\text{Dy}_6\text{Mn}_6(\text{H}_2\text{shi})_4(\text{Hshi})_2(\text{shi})_{10}(\text{MeOH})_{10}(\text{H}_2\text{O})_2]$ (**2**, $\text{H}_3\text{shi} = \text{salicylhydroxamic acid}$) complex, reported by Pecoraro.²⁰ These complexes presented no hysteresis down to 1.8 K, the temperature limit of commercial SQUID magnetometers, but ac magnetic susceptibility studies showed out-of-phase signals, as expected for SMM behaviour. Only for **1**(Tb) $[\text{CuLTb}(\text{hfac})_2]_2$ the maxima of the out-of-phase signals were observed above 1.8 K. In the same year, Christou and co-workers reported the first observed magnetization vs. field hysteresis loops for an heterometallic 3d-4f SMM²¹, a $[\text{Mn}_{11}\text{Dy}_4\text{O}_8(\text{OH})_6(\text{OMe})_2(\text{O}_2\text{CPh})_{16}(\text{NO}_3)_5(\text{H}_2\text{O})_3]$ complex, **3**. The out-of-phase ac magnetic susceptibility data showed no maxima down to 1.8 K but magnetization vs. field hysteresis loops were observed using a microsquid device below 1 K. The hysteresis loops were smooth, without the presence of the typical QTM steps signature of transition metal SMMs. This lack of steps in the magnetization vs. field hysteresis was attributed to a distribution of molecular environments or intermolecular interactions, both factors known to smooth or smear hysteresis loops in some transition metal SMMs.²² From these three first reports one can already take a clear conclusion: the ligands used are not specific for lanthanide-3d complexes, but are the usual varied ligands used in transition metal chemistry and lanthanide chemistry. Also from only these three reports one can see how in complex **2** the dysprosium ions are

close to each other and can be coupled, while in **1** and **3** the lanthanide ions are separated by the transition metals and could only couple to the transition metals.

The first results obtained seemed encouraging and efforts were doubled. In 2004 three peer reviewed research papers reported 3d-4f SMMs. From 2008 the number increased to between 10 and 16 papers each year reporting new 3d-4f SMMs. In 2014 the exponential growth in the field was reflected in more than 50 peer reviewed research papers reporting new 3d-4f SMMs. To the date of this report, 161 3d-4f SMMs have been reported. Nearly 2/3 of the reported 3d-4f SMMs contain Dy(III) as the lanthanide ion, and in most cases the coordination environment can be described as ligands on top and below the plane, thus providing the ideal setting for SMM properties for an oblate ion like Dy(III). One case of a neodymium 3d-4f complex, a $[\text{Mn}_4\text{Nd}_2]$ SMM, is reported, but no hysteresis was observed.⁷⁴ The 3d metal is usually Co(II) or Mn(III), both highly anisotropic, but also Fe(III), Ni(II), Cu(II) or even diamagnetic Co(III) and Zn(II). Worth to mention here are the reported 3d-4f SMMs that contain Gd(III) and La(III). In this two cases the lanthanide is either isotropic (Gd(III)) or diamagnetic (La(III)). All the reported 3d-4f SMMs reported with these two lanthanide ions are clearly cases where the anisotropy and the SMM property are both provided for by the 3d metal part of the complex.

By design: metal substitution

As in any polynuclear coordination complexes, the synthesis of 3d-4f SMMs follows most of the times a procedure of serendipitous self-assembly, where researchers try to provide the best reaction conditions to obtain complexes that might be new examples of SMMs. This is why there is such a rich structural diversity of 3d-4f SMMs, as is the case for transition metal SMMs. Of course the counterpart is the lack of control in the structure and properties of the prepared complexes. In the last few years the targeted substitution of a 3d metal by a lanthanide ion in a known transition metal polynuclear complex has been successfully done. This method has led to the isolation of 3d-4f complexes, where the position of the lanthanide ion could be predicted at the synthesis step. The first example was reported by Powell and co-workers in 2009,²³ when they succeeded in replacing the central Mn(II) atom of a ferromagnetically coupled $[\text{Mn}_{19}]^7$ complex, $[\text{Mn}_{19}\text{O}_8(\text{N}_3)_8(\text{HL})_{12}(\text{MeCN})_6]\text{Cl}_2$, with no anisotropy for a Dy(III) to obtain $[\text{Mn}_{18}\text{DyO}_8(\text{Cl})_{6.5}(\text{N}_3)_{1.5}(\text{HL})_{12}(\text{MeOH})_6]\text{Cl}_3$, (**4**). By this replacement retaining the core-topology of the cluster, the anisotropy of the complex was enhanced and the SMM property observed. Thus, the introduction of the anisotropic Dy(III) ion results in the onset of the SMM property, which was absent in $[\text{Mn}_{19}]$. Powell's complex **4** (Mn_{18}Dy) provided a sandwich type of ligand environment to the Dy(III) ion and thus complex **4** displayed SMM properties. $[\text{Mn}_{19}]$ was a record $S = 83/2$ spin but lacking any appreciable anisotropy. The

introduction of the Dy(III) ion in a sandwich like crystal field provided the necessary anisotropy to observe SMM behaviour. More recently we reported a $[\text{Mn}_7]$ species,²⁴ with a complex structure that was formed by three $[\text{Mn}(\text{II})_2]$ units centred around a Mn(II) ion in a very large cavity for a transition metal. Conditions were perfect for the controlled preparation of a Mn-Ln complex. We tweaked the reaction conditions and we successfully isolated the desired complexes $[\text{PrNH}_2]_3[\text{Mn}_6\text{LnO}_3(\text{OMe})_3(\text{SALO})_6(\text{SALOH})_3]$ with several lanthanide ions: La, Gd, Tb and Dy (**5**).¹⁰ The introduction of the lanthanide ion resulted in slightly enhanced SMM properties on **5**(La) and modified SMM properties for **5**(Dy) and **5**(Tb). In **5**(Gd) the SMM properties were completely quenched, probably due better magnetic coupling through the Gd(III) ion. In a qualitative, simple manner, this can be explained by looking at the coordination environment of the Ln(III) ion, which in the complexes **5**(Ln) was highly symmetrical resembling a spherical disposition of the ligands around the lanthanide, which according to Long's qualitative considerations should not provide a good crystal field for a bistable ground state for Dy(III) or Tb(III). In order to substitute a 3d metal for a lanthanide ion in a known complex there must be a metal site that is appropriate for the lanthanide. This is not straightforward and there are not many examples in the literature where controlled substitution is reported.

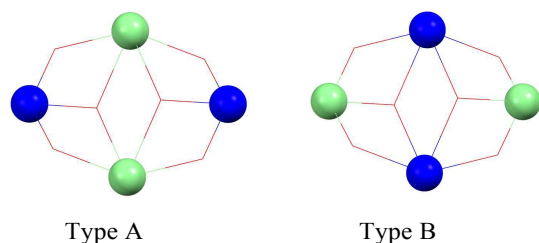


Figure 2. Ball and stick representation of the metal oxo core of a defective dicubane structure. The lanthanide ions are shown in green, the 3d metals are shown in blue.

Dy(III) 3d-4f SMMs

Without a doubt dysprosium is the most used lanthanide in order to obtain 3d-4f SMMs. The first reports in 2004 were of 3d-Dy SMMs. 3d-Dy SMMs have been reported for cobalt, chromium, copper, iron, manganese, nickel and zinc.

In several of these examples, the 3d metals in these species are Co(III) and Zn(II), thus, diamagnetic and it can be argued whether these must be considered 3d-4f SMMs or simply lanthanide SMMs with metalloligands, we decide to have these species here since usually when lanthanide SMMs are reviewed these species are not accounted for.²⁵ Chaudhury and co-workers propose to use diamagnetic Zn(II) ions in $[\text{M}_2(\text{L})_2(\text{PhCOO})_2\text{Dy}_2(\text{hfac})_4]$ (**6**(Zn) and **6**(Co) in Table 1) to enhance the energy barrier of Dy(III) SMMs as they show with DFT and ab-initio calculations, this is also studied by Shanmugam and co-workers.^{26,27} The record anisotropy barrier for 3d-4f SMMs belongs to a family of structurally related

$[\text{Co}(\text{III})_2\text{Dy}_2]$ complexes with double defective cubane structure prepared using tripodal ligands, the metal-oxo core is shown in Figure 2. This core-topology is well known in transition metal chemistry, and many $\text{Mn}(\text{II})_2\text{Mn}(\text{III})_2$ complexes have been reported with this core that are SMMs, a review of their properties and structures can be found in Aromi and Brechin's review.²⁸ The highest reported anisotropy barrier for a 3d-4f SMM belongs to a member of this family of complexes, with a Type A defective dicubane core as shown in Figure 2. $[\text{Co}_2\text{Dy}_2(\text{OMe})_2(\text{teaH})_2(\text{Piv})_6]$ (**7**, teaH = triethanolamine, Piv = pivalate)²⁹ displays two overlapped peaks in the out-of-phase ac magnetic susceptibility with $U_{\text{eff}} = 51$ and 127 K, shown in Figure 3. In 2013 and in 2014, Murray and co-workers reported two families of $[\text{Co}(\text{III})_2\text{Dy}(\text{III})_2]$ (**8** and **9** in Table 1) with metal arrangements of Type A as shown in Figure 2.^{30,31} This work added on their previous report of a $[\text{Ln}_2\text{Co}_2(\text{OMe})_2(\text{teaH})_2(\text{OOCPh})_4(\text{MeOH})_2(\text{NO}_3)_2]$ family of complexes in 2012³² with the same defective dicubane core. The dysprosium-cobalt analogue, $[\text{Dy}_2\text{Co}_2(\text{OMe})_2(\text{teaH})_2(\text{OOCPh})_4(\text{MeOH})_2(\text{NO}_3)_2]$ (complex **10** in Table 1) had a record energy barrier at the time of 88 K, and its ac data could be fit to a distribution of energy barriers with $\alpha = 0.25$ attributed by the authors to the fact that there are two independent Dy(III) sites.

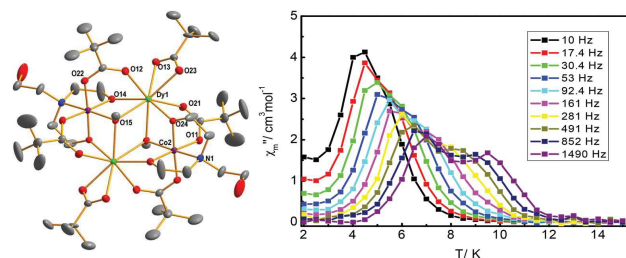


Figure 3. Crystal structure of $[\text{Co}_2\text{Dy}_2(\text{OMe})_2(\text{teaH})_2(\text{Piv})_6]$ (**6**) and out-of-phase ac susceptibility as a function of temperature, showing two overlapped peaks. Reproduced from reference 29 with permission from the Royal Society of Chemistry.

The authors were able to evaluate the magnetic exchange between Dy(III) ions, which was weak and antiferromagnetic. QTM was suppressed in a bulk sample of complex **10** due to the weak dipolar antiferromagnetic coupling, but dilution experiments in a yttrium(III) analogue matrix showed that fast tunnelling dominated the magnetic relaxation. The same authors showed how the structurally related $[\text{Cr}_2\text{Dy}_2(\text{OMe})_2(\text{Rdea})_2(\text{acac})_4(\text{NO}_3)_2]$ (Rdea: R-diethanolamine **11**(Me) R = methyl, **11**(Et) R = ethyl or **11**(tBu) R = tert-butyl) and $[\text{Cr}_2\text{Dy}_2(\text{OMe})_2(\text{mdea})_2(\text{O}_2\text{CPh})_4(\text{NO}_3)_2]$ (**12**) with Type A defective dicubane core as shown in Fig. 2 had large anisotropy barriers and long relaxation times compared to the Co(III) analogues due to the significant magnetic interaction between the 3d metal, Cr(III) and the lanthanide which suppresses QTM.³³ These Cr-Dy SMMs, **11**(Me), **11**(Et), **11**(tBu) and **12**

display hysteresis of the magnetization vs. applied field at temperatures as high as 2.2 K.

This core topology can also be found in the family $[\text{Ln}_2\text{Mn}_2(\text{OH})_2(\text{CymCOO})_8(\text{THF})_4]$ ($\text{Ln} = \text{Dy}$ **13**, Ho ; $\text{Cym} = (\mu_5\text{-C}_5\text{H}_4)\text{Mn}(\text{CO})_3$) where only the dysprosium analogue presents SMM properties.³⁴ In 2011 Powell and co-workers reported the Type B defective-dicubane complexes $[\text{Ni}_2\text{Ln}_2(\text{L})_4(\text{NO}_3)_2(\text{S})_2]$ ($\text{Ln} = \text{Dy}$ **14(S)**, Tb , $\text{L} = 2\text{-}(2\text{-hydroxy-3-methoxy-benzylideneamino})\text{phenol}$, $\text{S} = \text{MeOH}$ and DMF)³⁵ where the two dysprosium complexes, **14(MeOH)** and **14(DMF)** are SMMs and the blocking temperature seems to be modulated by the coordination environment around the Ni(II) ions. The structure of these complexes is somehow different from the SMMs reported by Murray and co-workers, now the dysprosium ions are not part of the central $[\text{M}_2\text{O}_2]$ unit, but at the tips of the molecule resulting in two fairly well separated ions, nearly magnetically independent. In 2012 the same group reported $[\text{Co}_2\text{Dy}_2(\text{L})_4(\text{NO}_3)_2(\text{THF})_2]$ (**15**),³⁶ Type B defective-dicubanes, which was also a SMM. Cobalt is in the oxidation state Co(II), paramagnetic. The authors show how single-ion blocking of the Dy(III) ions occurs at higher temperatures with a crossover to molecular exchanged-based blocking at low temperatures. For **15** there are two differentiated thermally activated regimes with effective barriers of 82 and 11 K, respectively. Hysteresis loops were clearly observed up to 3 K. In this very interesting paper the authors unambiguously assign the large energy barrier to the relaxation of the Dy(III) ions and the low temperature behaviour to the exchange-blocked relaxation where the 3d-4f coupling dominates.

A number of higher nuclearity 3d-4f complexes have been reported, many of them are SMMs with diverse structures and ligands. Most of these have relatively small energy barriers. An exception is an enneanuclear complex $[\text{Mn}_5\text{Dy}_4\text{O}_6(\text{mdea})_2(\text{mdeaH})_2(\text{Piv})_6(\text{NO}_3)_4(\text{H}_2\text{O})_2]$ (**16(Dy)**) reported by Powell et al, the complex possesses an energy barrier of 38.6 K and displays hysteresis vs. field magnetization loops up to 1.9 K.³⁷ The Tb(III), Ho(III) and Y(III) (**16(Tb)**, **16(Ho)** and **16(Y)**) analogues are also SMMs, but with smaller energy barriers. The diamagnetic Y(III) analogue highlights the fact that the Mn_5 unit also contributes to the SMM behaviour.

The $[\text{Mn}_{21}\text{DyO}_{20}(\text{OH})_2(\text{tBuCOO})_{20}(\text{HCO}_2)_4(\text{NO}_3)_3(\text{H}_2\text{O})_7]$ complex, (**17**) shown in Fig. 4, reported by Christou and co-workers in 2011 also shows hysteresis of the magnetization up to 3 K and has a large energy barrier of 74 K.³⁸ In complex **17** a single Dy(III) is at one vertex of a $[\text{M}_4\text{O}_4]$ cubane, which is surrounded by a Mn-O core which is probably a strong contributor to the SMM properties. The 3d-4f SMM containing the largest number of Dy(III) ions is complex **18** with ten Dy(III) and two cobalt ions $[\text{Dy}_{10}\text{Co}_2(\text{L})_4(\text{MeCOO})_{16}(\text{SCN})_2(\text{MeCN})_2(\text{H}_2\text{O})_4(\text{OH})_6] \cdot 2\text{Co}(\text{SCN})_4$, reported in 2011 by Tang and his group.³⁹ Complex **18** contains ten dysprosium ions and two Co(II) in a wheel-like

arrangement. Below 10 K the authors report slow relaxation with a crossover from single ion relaxation due to the Dy(III) centres to the exchanged coupled system. Two complexes have been reported with eight dysprosium ions. $[\text{H}_3\text{O}][\text{Cu}_{24}\text{Dy}_8(\text{Ph}_3\text{CPO}_3)_6(\text{Ph}_3\text{CPO}_3\text{H})_6(\text{MeCOO})_{12}(\text{MeCOOH})_6(\text{OH})_{42}(\text{NO}_3)(\text{OH}_2)_6]$ (**19**) was reported in 2010 by Winpenny and co-workers.⁴⁰ The Gd(III) analogue is not an SMM, thus the anisotropy is provided by the eight dysprosium ions. As usual for very large complexes the blocking temperature is very low (0.6 K) and the hysteresis loops M vs. H are smooth. The same year Murray and co-workers reported complex **20** with nine Mn(III) and eight dysprosium ions, $[\text{Mn}_9\text{Dy}_8\text{O}_8(\text{OH})_8(\text{tea})_2(\text{teaH})_2(\text{teaH}_2)_4(\text{MeCOO})_4(\text{NO}_3)_2(\text{H}_2\text{O})_4](\text{NO}_3)_7$.⁴¹ Complex **20** is an SMM but no maxima in the ac susceptibility were observed. Again, the largest nuclearity complexes fail to provide the best magnetic properties. In 2015 Tang and co-workers report Mn(II)-Ln2 SMMs with the Dy(III) analogue, **41(Dy)** displaying a large $U_{\text{eff}} = 92$ K.⁷³

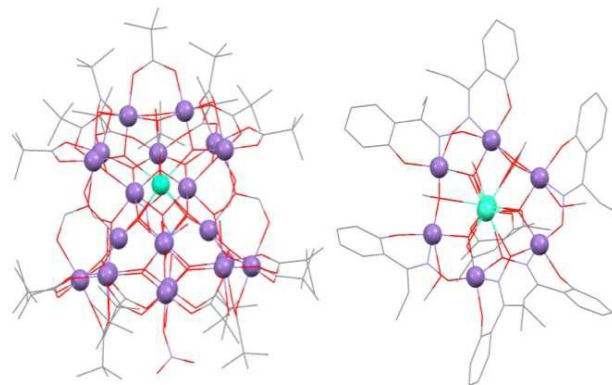


Figure 4. Crystal structures of some 3d-4f SMMs: (left) $[\text{Mn}_{21}\text{DyO}_{20}(\text{OH})_2(\text{tBuCOO})_{20}(\text{HCO}_2)_4(\text{NO}_3)_3(\text{H}_2\text{O})_7]$ (**17**) from reference 38; (right) **21(Tb)** $[\text{Mn}_6\text{O}_3(\text{saO})_6(\text{MeO})_6\text{Tb}_2(\text{MeOH})_4(\text{H}_2\text{O})_2]$ from reference 45.

Tb 3d-4f SMMs

Terbium(III) is the lanthanide ion that has provided the mononuclear SMM complexes with record effective energy barriers⁴²⁻⁴⁴ due to the large separation of the m_f sublevels and the large anisotropy characteristic of terbium(III). However, terbium is a non-Kramer's ion and the ground state will only be bi-stable in axial-symmetry ligand fields. Thus, there are much less Tb(III) SMMs reported than Dy(III) SMMs. For 3d-4f SMMs this picture still holds: for every two 3d-Dy SMM reported complexes there is only one 3d-Tb SMM. The terbium analogues of 3d-Dy SMMs most of the times do not display SMM properties or are worse SMMs than the dysprosium analogues. SMMs containing Tb have been reported mostly for copper and manganese, but also with nickel, cobalt, iron and chromium. The ones with highest energy barriers are manganese-terbium complexes. In 2011 Dehnen and co-workers reported the octanuclear complex **21(Tb)** $[\text{Mn}_6\text{O}_3(\text{saO})_6(\text{MeO})_6\text{Tb}_2(\text{MeOH})_4(\text{H}_2\text{O})_2]$ with an energy

barrier of 103 K.⁴⁵ This complex displayed a high blocking temperature of 3.1 K. The lanthanum analogue, **21**(La) was also an SMM with a large blocking temperature and relatively large energy barrier of 32 K. Brechin and co-workers reported the same year complex **22**(Gd) with similar core, [Gd₂Mn₆O₃(OMe)₄(Et-sao)₆(acac)₂(MeOH)₄] but different ligands and an energy barrier of 24 K.⁴⁶ The energy barrier was also high for the terbium complex **22**(Tb), U_{eff} = 46 K. In this case clearly the anisotropy of the terbium ion has actually boosted the SMM properties of the [Mn₆] unit, showing how the right combination of anisotropic 3d metal and anisotropic lanthanide can lead to better, improved SMMs. The high nuclearity, high symmetry (D₂) complex **23**(Tb) reported by Tong and co-workers [Tb₆Mn₁₂O₇(OH)₁₀(OAc)₁₄(mpea)₈]⁴⁷ has an energy barrier of U_{eff} = 36.6 K. A related complex, which differs in some of the terminal ligands and the orientation of the two related [Ln(III)₃] units, complex **24** [Tb₆Mn₁₂O₉(OH)₈(OAc)₁₀(mpea)₈(mp)₂(MeOH)₂(H₂O)₂] has lower symmetry (C₁) and a smaller energy barrier value of 19.6 K. In this particular case, the dysprosium analogue **23**(Dy) has smaller anisotropy barrier. Complex **25**, [Mn₅Tb₄O₆(mdea)₂(mdeaH)₂(Piv)₆(NO₃)₄(H₂O)₂] reported by Powell and co-workers with a core of two distorted [Mn(IV)Mn(III)Tb₂O₄] cubanes sharing a Mn(IV) vertex has an energy barrier of the same order (33 K).³⁷ Another example with even smaller anisotropy barrier is complex **26**(Tb) [Mn₃Tb₄(mosao)₂(mosaoH)₄(piv)₄(N-mdea)₄], consisting of two triangles of [Mn(III)Tb₂] linked to a central Mn(II) atom, the analogue with diamagnetic Y, **26**(Y) has an energy barrier of 13.8 K generated by the anisotropy and spin of the manganese unit.⁴⁸

There are several 3d-Tb SMM synthesized with Cu, the most relevant is complex **27** [TbCu₄(L)₂(OH)₄(H₂O)₈(NO₃)](ClO₄)₂ with U_{eff} = 25 K is a tetragonal pyramid with a large and flexible ligand bis(-carboxyethyl)isocyanurate.⁴⁹ On the other hand, we can see an example of a family of trinuclear [Cu₂Tb] complexes like [(CuL)₂Tb(H₂O)(NO₃)₃] (**28**) or [{(CuL)₂Tb(H₂O)(NO₃)₃}₂bpy] (**29**) with different assemblies showing values of anisotropy barrier between 18 K and 23 K.⁵⁰ One-dimensional chain of units like that of complexes **28** and **29** behave as a single chain magnet (SCM).^{50,51} Two more examples of Cu-Tb SMMs are complex **30** [TbCu₃(H₂edte)(NO₃)](NO₃)₂,⁵² or complex **31** [Cu₃Tb(L^{bu})(NO₃)₂(MeOH)(H₂O)](NO₃) with an hexamine macrocycle ligand.⁵³ Complex **32** is a rare example of a heterotrimetallic coordination complex of formula [Cu(H₂L)(MeOH)]₂Tb(H₂O)_{0.57}(DMF)_{0.43}Fe(CN)₆ exhibiting an energy barrier of 13 K.⁵⁴ Some other SMMs reported on the bibliography are an octanuclear complex [Cu₆Tb₂(L³⁻)₄(NO₃)₃(OAc)₂(MeOH)₅]NO₃, complex **33** is described as an oblate wheel that has an energy barrier of 15.6 K⁵⁵ or complex **34**, a dinuclear Cu-Tb complex,

[LCu(O₂COMe)Tb(thd)₂], with a Schiff base ligand with U_{eff} = 13 K.⁵⁶

Complex [Tb₂Ni₄L₂Cl₂(OH)₂(MeO)₂(MeOH)₆]Cl₂(ClO₄)₂ **35**(Tb) is a defect cubane complex with Schiff-base ligands. Complex **35**(Tb) exhibits an anisotropy barrier of 30 K. The magnetic data obtained with the Ni-Y(III) analogue **35**(Y) demonstrated that the 4f metal contribution to the SMM properties was dominant.⁵⁷ Complex **36** is another rare heterotrinuclear 3d-4f-5d complex containing tungsten⁵⁸ [LM₂Ni(H₂O)Tb(dmf)_{2.5}(H₂O)_{1.5}]{W(CN)₈} showing an anisotropy barrier of 15 K. It is worth to point out that none of the reported 3d-Tb(III) SMMs report magnetization vs. field hysteresis loops above 2.0 K.

Sm, Ho, Er and Yb 3d-4f SMMs

Even though dysprosium and terbium are undoubtedly the two lanthanide ions that have provided better SMMs there are some interesting examples with other lanthanide ions. Samarium, with a less than half filled shell and the smallest J as ground state is rarely present in SMMs. According to the observations of Long and Rinehart, a mostly equatorial arrangement of ligands would be required to provide a bi-stable ground state for an isolated Sm(III) ion. This ligand arrangement is not very common. In 2010 Bu and co-workers reported the first Sm-3d SMM, [Fe₁₂Sm₄O₁₀(OH)₄(PhCO₂)₂₄] (**37**(Sm)).⁵⁹ Complex **37**(Sm) contained twelve Fe(III) ions and four Sm(III) with an effective barrier of 16 K and a blocking temperature of 0.5 K. In **37**(Sm) each Sm(III) ion is interacting with five iron centres and one samarium via monoatomic oxo bridges. The [Fe₁₂] unit of the cluster possesses a large spin ground state, but **37**(Gd) is not an SMM. The large spin of the [Fe₁₂] part of the cluster combined with a ligand arrangement around the samarium in an unusual muffin like geometry with five ligands around the Sm(III) ion in an equatorial fashion result in a bi-stable ground state. Since the magnetic moment of samarium is not large, even with the ideal ligand field, the [Fe₁₂Sm₄] complex **37**(Sm) is not a very good SMM. In 2014 the same group reported new members of the same family of [Fe₁₂Sm₄] SMMs, with similar magnetic properties.⁶⁰ In 2010 Powell and co-workers reported a family of [Mn(III)₄Ln(III)] complexes, **38**. **38**(Sm) [Mn₄Sm₄(nBudea)₄(HCOO)₄(OMe)₄(OOCe)₈(MeOH)₄] was an SMM with an energy barrier of 12 K when an applied dc field of 2000 Oe was used to suppress QTM.⁶¹ The yttrium analogue **38**(Y) also presents slow relaxation of the magnetization, highlighting the importance of the [Mn(III)₄] part of the cluster in the slow relaxation behaviour. The complex **27**(Sm) [SmCu₄(L)₂(OH)₄(H₂O)₈(NO₃)](ClO₄)₂ reported in 2012 analogue to **27**(Tb) is also SMM.⁴⁹ Two papers report 3d-Er SMMs^{62,63} and there are eight 3d-Ho SMMs.^{64-68,34,57,69} All of them display very small energy barriers and no reported blocking temperatures. Some of these are part of families of SMMs, were the usually the Dy and Tb analogues display better SMM properties.

Two ytterbium 3d-4f SMMs, **39** and **40** in Table 1, were reported in 2014 by Brechin et al.⁷⁰ These were the two first 3d-4f SMMs of Yb(III) but the 3d metal was Zn(II), diamagnetic. Ac out-of-phase susceptibility peaks were observed when applying a 1000 Oe dc field, something usual for Yb(III) SMMs. The interest of these species was focused on a combination of SMM and luminescent properties, associated to Yb(III).

Challenges ahead and concluding remarks

The biggest challenge remains still to rise the blocking temperature of the new SMMs, no matter whether we talk about transition metals, 4f or 3d-4f SMMs. We have included here some complexes that are claimed as SMMs but for which no maxima in the out-of-phase ac magnetic susceptibility or hysteresis of the magnetization vs. field are reported. Clearly, the limited access to experiments at temperatures below 2 K is an obstacle in this respect. However, we expect that when new 3d-4f SMMs with higher blocking temperatures are reported this fact ceases to be a problem and there will be less ambiguity as to the physical properties of reported species: both ac magnetic susceptibility out-of-phase maxima and magnetization vs. field hysteresis should be observed to claim a complex is an SMM. With lanthanide SMMs the effective energy barriers have been greatly increased, up to hundreds of kelvin in several mononuclear SMMs Tb-phthalocyanine derivatives pure or doped in diamagnetic yttrium matrices,²⁵ but this has not been accompanied by a real increase in blocking temperatures thus hampering potential application of lanthanide SMMs. This problem might be overcome by 3d-4f SMMs. Several examples report large effective energy barriers (at least of the order of those reported for 3d SMMs) that are in a few cases accompanied by relatively high blocking temperatures, such as those reported by Murray and co-workers for [Cr₂Dy₂] SMMs, with TB = 2.2 K and particularly relevant, the [Mn₆Tb₂] reported by Dehnen and co-workers with U_{eff} = 103 K and TB = 3.5 K.^{33,45} The Cr(III)-Dy(III) significant magnetic interaction is claimed to be the key factor in quenching QTM and it is directly related to the anisotropy barrier, thus opening up a challenging new route to control SMM properties of Cr(III)-Dy(III) ions. Could this be exploited for other 3d-4f SMMs? It is still a big synthetic challenge to prepare 3d-4f complexes with strong magnetic coupling between the 3d and 4f ions, but this might be a great goal to have in mind. The synthetic methods clearly offer a rich variety of products, with different levels of control on the design of the prepared complexes. There is not a clear picture of preferred ligands to prepare 3d-4f SMMs, and complexes are reported with all kinds of ligand types, but poly-alcoxo and Schiff bases of salicylaldehyde appear in many of the reported complexes.

The advances on the theoretical understanding of the magnetic properties of the lanthanide ions and their 3d-4f complexes are still lagging behind the advances in the synthesis of new

complexes. There is still a lot to learn about heterometallic 3d-4f complexes, especially about the magnetic coupling between 3d and 4f metals. We strongly believe the study of 3d-4f interactions as it becomes more common, even in dinuclear model complexes, will provide good ideas for the design of new 3d-4f SMMs. From the knowledge base of 3d-4f SMMs reported up to 2014, dysprosium seems to be the best lanthanide to provide 3d-4f SMMs. Furthermore, two main trends of design of new 3d-4f SMMs emerge as the most plausible to provide better 3d-4f SMMs in the near future: isolated lanthanide ions with a 3d metalloligand, as the [Mn₂Dy] reported by Christou and co-workers,³⁸ with TB = 3.0 K, or 3d-4f complexes with strong magnetic coupling between the metals to suppress QTM. Also a combination of these approaches emerges as a good option: a 3d-4f SMM with strong coupling between a unique lanthanide ion and a 3d metalloligand with large S that would help in quenching the QTM thus increasing the blocking temperature.

Acknowledgements

ECS and LRP acknowledge the financial support from the Spanish Government, (Grant CTQ2012-32247).

Notes and references

^a Departament de Química Inorgànica i Institut de Nanociència i Nanotecnologia, Universitat de Barcelona. Av. Diagonal 645, 08028 Barcelona, SPAIN. Email: esanudo@ub.edu
DOI: 10.1039/b000000x/

1. R. Sessoli, H.-L. Tsai, A. R. Schake, S. Wang, J. B. Vincent, K. Folting, D. Gatteschi, G. Christou, and D. N. Hendrickson, *J. Am. Chem. Soc.*, 1993, **115**, 1804–1816.
2. N. E. Chakov, S. Lee, A. G. Harter, P. L. Kuhns, A. P. Reyes, S. O. Hill, N. S. Dalal, W. Wernsdorfer, K. A. Abboud, and G. Christou, *J. Am. Chem. Soc.*, 2006, **128**, 6975–6989.
3. C. J. Milios, A. Vinslava, W. Wernsdorfer, S. Moggach, S. Parsons, S. P. Perlepes, G. Christou, and E. K. Brechin, *J. Am. Chem. Soc.*, 2007, **129**, 2754–2755.
4. E. K. Brechin, C. Boskovic, W. Wernsdorfer, J. Yoo, A. Yamaguchi, E. C. Sanudo, T. R. Concolino, A. L. Rheingold, H. Ishimoto, D. N. Hendrickson, and G. Christou, *J. Am. Chem. Soc.*, 2002, **124**, 9710–9711.
5. E. C. Sañudo, W. Wernsdorfer, K. A. Abboud, and G. Christou, *Inorg. Chem.*, 2004, **43**, 4137–4144.
6. A. J. Tasiopoulos, A. Vinslava, W. Wernsdorfer, K. a Abboud, and G. Christou, *Angew. Chem. Int. Ed. Engl.*, 2004, **43**, 2117–2121.
7. A. M. Ako, I. J. Hewitt, V. Mereacre, R. Clérac, W. Wernsdorfer, C. E. Anson, and A. K. Powell, *Angew. Chem. Int. Ed. Engl.*, 2006, **45**, 4926–4929.
8. N. Ishikawa, M. Sugita, T. Ishikawa, S.-Y. Koshihara, and Y. Kaizu, *J. Am. Chem. Soc.*, 2003, **125**, 8694–8695.
9. J. D. Rinehart and J. R. Long, *Chem. Sci.*, 2011, **2**, 2078–2085.
10. M. Ledezma-Gairaud, L. Grangel, G. Aromí, T. Fujisawa, A. Yamaguchi, A. Sumiyama, and E. C. Sañudo, *Inorg. Chem.*, 2014, **53**, 5878–5880.

11. E. C. Sañudo, C. A. Muryn, M. A. Helliwell, G. A. Timco, W. Wernsdorfer, and R. E. P. Winpenny, *Chem. Commun.*, 2007, 801–803.
12. N. F. Chilton, R. P. Anderson, L. D. Turner, A. Soncini, and K. S. Murray, *J. Comput. Chem.*, 2013, **34**, 1164–1175.
13. J. Dreiser, K. S. Pedersen, C. Piamonteze, S. Rusponi, Z. Salman, M. E. Ali, M. Schau-Magnussen, C. A. Thuesen, S. Piligkos, H. Weihe, H. Mutka, O. Waldmann, P. Oppeneer, J. Bendix, F. Nolting, and H. Brune, *Chem. Sci.*, 2012, **3**, 1024–1032.
14. M. Chen, E. C. Sañudo, E. Jiménez, S.-M. Fang, C.-S. Liu, and M. Du, *Inorg. Chem.*, 2014, **53**, 6708–6714.
15. M. Mannini, P. Sainctavit, R. Sessoli, C. Cartier dit Moulin, F. Pineider, M.-A. Arrio, A. Cornia, and D. Gatteschi, *Chem. Eur. J.*, 2008, **14**, 7530–7535.
16. M. Mannini, F. Pineider, C. Danieli, F. Totti, L. Sorace, P. Sainctavit, M. Arrio, E. Otero, L. Joly, J. C. Cezar, A. Cornia, and R. Sessoli, *Nature*, 2010, **468**, 417–421.
17. L. Malavolti, V. Lanzilotto, S. Ninova, L. Poggini, I. Cimatti, B. Cortigiani, L. Margheriti, D. Chiappe, E. Otero, P. Sainctavit, F. Totti, A. Cornia, M. Mannini, and R. Sessoli, *Nano Lett.*, 2015, **15**, 535–541.
18. R. Sessoli, M. Mannini, F. Pineider, A. Cornia, and P. Sainctavit, *Magnetism and Synchrotron Radiation*, Springer Berlin Heidelberg, Berlin, Heidelberg, 2010, vol. 133.
19. S. Osa, T. Kido, N. Matsumoto, N. Re, A. Pochaba, and J. Mrozinski, *J. Am. Chem. Soc.*, 2004, **126**, 420–421.
20. C. M. Zaleski, E. C. Depperman, J. W. Kampf, M. L. Kirk, and V. L. Pecoraro, *Angew. Chem. Int. Ed. Engl.*, 2004, **43**, 3912–3914.
21. A. Mishra, W. Wernsdorfer, K. A. Abboud, and G. Christou, *J. Am. Chem. Soc.*, 2004, **126**, 15648–15649.
22. E. C. Sañudo, W. Wernsdorfer, K. A. Abboud, and G. Christou, *Inorg. Chem.*, 2004, **43**, 4137–4144.
23. A. M. Ako, V. Mereacre, R. Clérac, W. Wernsdorfer, I. J. Hewitt, C. E. Anson, and A. K. Powell, *Chem. Commun.*, 2009, 544–546.
24. M. Ledezma-Gairaud, L. W. Pineda, G. Aromí, and E. C. Sañudo, *Polyhedron*, 2013, **64**, 45–51.
25. (a) D. N. Woodruff, R. E. P. Winpenny, and R. A. Layfield, *Chem. Rev.*, 2013, **113**, 5110–5148; (b) P. Zhang, Y.-N. Guo, J. Tang, *Coord. Chem. Rev.* 2013, **257**, 1728–1763; (c) P. Zhang, L. Zhang, J. Tang, *Dalton Trans.* 2015, **44**, 3923–3929.
26. S. T. Abtab, M. C. Majee, M. Maity, J. Titis, R. Boca, and M. Chaudhury, *Inorg. Chem.*, 2014, **53**, 1295–1306.
27. A. Upadhyay, S. K. Singh, C. Das, R. Mondol, S. K. Langley, K. S. Murray, G. Rajaraman, and M. Shanmugam, *Chem. Commun.*, 2014, **50**, 8838–8841.
28. G. Aromí and E. K. Brechin, in *Structure and Bonding*, Springer-Verlag, Berlin, 2006, pp. 1–67.
29. A. V Funes, L. Carrella, E. Rentschler, and P. Alborés, *Dalt. Trans.*, 2014, **43**, 2361–2364.
30. S. K. Langley, N. F. Chilton, B. Moubaraki, and K. S. Murray, *Inorg. Chem.*, 2013, **52**, 7183–7192.
31. S. K. Langley, L. Ungur, N. F. Chilton, B. Moubaraki, L. F. Chibotaru, and K. S. Murray, *Inorg. Chem.*, 2014, **53**, 4303–4315.
32. S. K. Langley, N. F. Chilton, L. Ungur, B. Moubaraki, L. F. Chibotaru, and K. S. Murray, *Inorg. Chem.*, 2012, **51**, 11873–11881.
33. S. K. Langley, D. P. Wielechowski, V. Vieru, N. F. Chilton, B. Moubaraki, L. F. Chibotaru, and K. S. Murray, *Chem. Sci.*, 2014, **5**, 3246–3256.
34. P. S. Koroteev, N. N. Efimov, A. B. Ilyukhin, Z. V. Dobrokhotova, and V. M. Novotortsev, *Inorganica Chim. Acta*, 2014, **418**, 157–162.
35. K. C. Mondal, G. E. Kostakis, Y. Lan, W. Wernsdorfer, C. E. Anson, and A. K. Powell, *Inorg. Chem.*, 2011, **50**, 11604–11611.
36. K. C. Mondal, A. Sundt, Y. Lan, G. E. Kostakis, O. Waldmann, L. Ungur, L. F. Chibotaru, C. E. Anson, and A. K. Powell, *Angew. Chem. Int. Ed. Engl.*, 2012, **51**, 7550–7554.
37. V. Mereacre, A. M. Ako, R. Clérac, W. Wernsdorfer, I. J. Hewitt, C. E. Anson, and A. K. Powell, *Chem. Eur. J.*, 2008, **14**, 3577–3584.
38. C. Papatriantafyllopoulou, W. Wernsdorfer, K. A. Abboud, and G. Christou, *Inorg. Chem.*, 2011, **50**, 421–423.
39. L.-F. Zou, L. Zhao, Y.-N. Guo, G.-M. Yu, Y. Guo, J. Tang, and Y.-H. Li, *Chem. Commun.*, 2011, **47**, 8659–8661.
40. V. Baskar, K. Gopal, M. A. Helliwell, F. Tuna, W. Wernsdorfer, and R. E. P. Winpenny, *Dalt. Trans.*, 2010, **39**, 4747–4750.
41. S. K. Langley, B. Moubaraki, and K. S. Murray, *Dalt. Trans.*, 2010, **39**, 5066–5069.
42. S. Takamatsu, T. Ishikawa, S. Koshihara, and N. Ishikawa, *Inorg. Chem.*, 2007, **46**, 7250–7252.
43. F. Branzoli, P. Carretta, M. Filibian, G. Zoppellaro, M. J. Graf, J. R. Galan-Mascaros, O. Fuhr, S. Brink, and M. Ruben, *J. Am. Chem. Soc.*, 2009, **131**, 4387–4396.
44. M. Gonidec, R. Biagi, V. Corradini, F. Moro, V. De Renzi, U. Pennino, D. Summa, L. Muccioli, C. Zannoni, D. B. Amabilino, and J. Veciana, *J. Am. Chem. Soc.*, 2011, **133**, 6603–6612.
45. M. Holyńska, D. Premužić, I.-R. Jeon, W. Wernsdorfer, R. Clérac, and S. Dehnen, *Chemistry*, 2011, **17**, 9605–9610.
46. G. Rigaux, R. Inglis, S. Morrison, A. Prescimone, C. Cadiou, M. Evangelisti, and E. K. Brechin, *Dalton Trans.*, 2011, **40**, 4797–4799.
47. J. Liu, W. Lin, Y. Chen, J. Leng, F. Guo, and M. Tong, *Inorg. Chem.*, 2013, **52**, 457–463.
48. H. Chen, C.-B. Ma, M.-Q. Hu, H.-M. Wen, and C.-N. Chen, *Dalton Trans.*, 2014, **43**, 16737–16744.
49. Q. Zhu, S. Xiang, T. Sheng, D. Yuan, C. Shen, C. Tan, S. Hu, and X. Wu, *Chem. Commun.*, 2012, **48**, 10736–10738.
50. S. Ghosh, Y. Ida, T. Ishida, and A. Ghosh, *Cryst. Growth Des.*, 2014, **14**, 2588–2598.
51. Z.-X. Wang, X. Zhang, Y.-Z. Zhang, M.-X. Li, H. Zhao, M. Andruh, and K. R. Dunbar, *Angew. Chem. Int. Ed. Engl.*, 2014, **53**, 11567–11570.
52. F. J. Kettles, V. A. Milway, F. Tuna, R. Valiente, L. H. Thomas, W. Wernsdorfer, S. T. Ochsenein, and M. Murrie, *Inorg. Chem.*, 2014, **53**, 8970–8978.
53. H. L. C. Feltham, R. Clerac, L. Ungur, L. F. Chibotaru, A. K. Powell, and S. Brooker, *Inorg. Chem.*, 2013, **52**, 3236–3240.
54. K.-Q. Hu, S.-Q. Wu, A.-L. Cui, and H.-Z. Kou, *Transit. Met. Chem.*, 2014, **39**, 713–718.

55. S. Xue, Y. Guo, L. Zhao, H. Zhang, and J. Tang, *Inorg. Chem.*, 2014, **53**, 8165–8171.
56. J. Costes, F. Dahan, and W. Wernsdorfer, *Inorg. Chem.*, 2006, **45**, 5–7.
57. L. Zhao, J. Wu, H. Ke, and J. Tang, *Inorg. Chem.*, 2014, **53**, 3519–3525.
58. J. Sutter, S. Dhers, R. Rajamani, S. Ramasesha, J. P. Costes, C. Duhayon, and L. Vendier, *Inorg. Chem.*, 2009, **48**, 5820–5828.
59. Y.-F. Zeng, G.-C. Xu, X. Hu, Z. Chen, X.-H. Bu, S. Gao, and E. C. Sañudo, *Inorg. Chem.*, 2010, **49**, 9734–9736.
60. S.-J. Liu, Y.-F. Zeng, L. Xue, S.-D. Han, J.-M. Jia, T.-L. Hu, and X.-H. Bu, *Inorg. Chem. Front.*, 2014, **1**, 200–206.
61. M. Li, Y. Lan, A. M. Ako, W. Wernsdorfer, C. E. Anson, G. Buth, A. K. Powell, Z. Wang, and S. Gao, *Inorg. Chem. (Washington, DC, United States)*, 2010, **49**, 11587–11594.
62. D. R. Turner, K. J. Berry, N. F. Chilton, B. Moubaraki, K. S. Murray, G. B. Deacon, and S. R. Batten, *Dalt. Trans.*, 2012, **41**, 11402–11412.
63. H. Chen, C. Ma, M. Hu, H. Wen, H. Cui, J.-Y. Liu, X.-W. Son, and C.-N. Chen, *Dalt. Trans.*, 2013, **42**, 4908–4914.
64. V. Chandrasekhar, B. M. Pandian, J. J. Vittal, and R. Clerac, *Inorg. Chem.*, 2009, **48**, 1148–1157.
65. S. K. Langley, L. Ungur, N. F. Chilton, B. Moubaraki, L. F. Chibotaru, and K. S. Murray, *Chem. Eur. J.*, 2011, **17**, 9209–9218.
66. M. Murugesu, A. Mishra, W. Wernsdorfer, K. A. Abboud, and G. Christou, *Polyhedron*, 2006, **25**, 613–625.
67. N. Ahmed, C. Das, S. Vaidya, S. K. Langley, K. S. Murray, and M. Shanmugam, *Chemistry (Easton)*, 2014, **20**, 14235–14239.
68. F. Gao, L. Cui, Y. Song, Y.-Z. Li, and J.-L. Zuo, *Inorg. Chem.*, 2014, **53**, 562–567.
69. P. Bag, A. Chakraborty, G. Rogez, and V. Chandrasekhar, *Inorg. Chem.*, 2014, **53**, 6524–6533.
70. J. Ruiz, G. Lorusso, M. Evangelisti, E. K. Brechin, S. J. A. Pope, and E. Colacio, *Inorg. Chem.*, 2014, **53**, 3586–3594.
71. Y.-N. Guo, G.-F. Xu, Y. Guo, J. Tang, *Dalton Trans.* 2011, **40**, 9953–9963.
72. L. Ungur, S.-Y. Lin, J. Tang, L. F. Chibotaru, *Chem. Soc. Rev.* 2014, **43**, 6894–6905.
73. X.L. Li, F.-Y. Min, C. Wang, S.-Y. Lin, Z. Liu, J. Tang, *Dalton Trans.* **44**, 3430–3438.
74. H. Ke, L. Zhao, Y. Guo, J. Tang, *Dalton Trans.* 2012, **41**, 2314–2319.